Journal of Materials Chemistry C

Accepted Manuscript

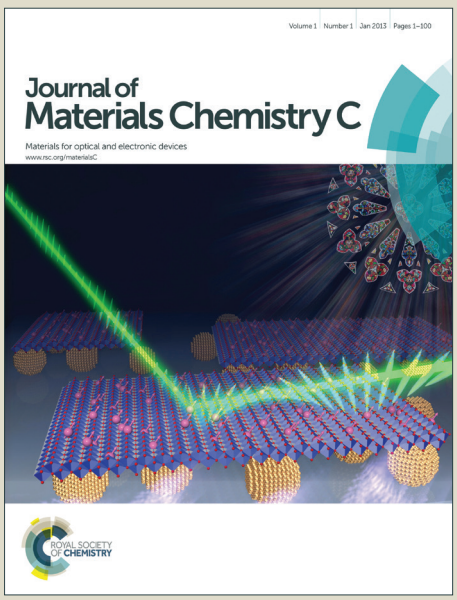

ROYAL SOCIETY OF CHEMISTRY

www.rsc.org/materialsC

Journal of Materials Chemistry C

Journal of Materials Chemistry C

Dynamic Article Links ►

Cite this: DOI: 10.1039/c0xx00000x

ARTICLE TYPE

www.rsc.org/xxxxxx

Encapsulating carbon nanotubes with SiO_2: a strategy of applying them in polymer nanocomposites with high mechanical strength and electrical insulation

Xiaoliang Zeng,[a,b] Shuhui Yu, [a] * Lei Ye,[c] Mingyang Li,[a] Zhilong Pan,[a] Rong Sun,[a] * and Jianbin Xu[c]

Received (in XXX, XXX) Xth XXXXXXXXX 20XX, Accepted Xth XXXXXXXXX 20XX
DOI: 10.1039/b000000x

Multiwalled carbon nanotubes (MWCNTs) have been widely used as mechanical reinforcement fillers for polymer during the past decades. However, high electrical conductivity of MWCNTs hampers their applications in some special fields. In this study, the MWCNT was encapsulated with an insulating silicon oxide (SiO_2) layer to form core-shell structure MWCNT@SiO_2 nanoparticles, which were used to fill bismaleimide-triazine (BT) resin. The obtained polymer nanocomposites possessed high mechanical strength, electrical insulation, improved thermal stability, and good optical transparency. These excellent properties were attributed to the strong interfacial interaction between MWCNT@SiO_2 and polymer, as well as the suppression of electron transport by SiO_2 layer on MWCNT surface. The nanocomposites were employed to fabricate a printed circuit substrate, on which a frequency "flasher" circuit and the electrical components worked well. This work has demonstrated the possibility of using MWCNTs as mechanical reinforcement fillers in polymer nanocomposites, which simultaneously possess electrical insulation.

1. Introduction

Polymer nanocomposites have received a great deal of attention both in science and engineering over recent decades in the development of advanced materials for a wide range of applications.[1] Carbon nanotubes (CNTs) have been considered to be ideal reinforcement fillers for high-performance polymer nanocomposites due to their excellent mechanical properties, involving excellent Young's module with values greater than 1 TPa and tensile strength of 63 GPa. [2] A small addition amount of CNTs to polymers could result in superior mechanical properties, as previously reported.[3-6] On the other hand, owing to their intrinsic nature, the addition of CNTs simultaneously leads to enhanced electrical conductivity, even at low volume fractions[7-11]. The electrically conductive polymer nanocomposites are regarded as promising materials for use in sensors, actuators, and electromagnetic shielding, etc.[12-14] However, high electrical conductivity hampers their application in some fields, such as printed circuit substrates, sealants for semiconductor devices and light emitting diodes, etc.

In order to utilize the outstanding mechanical strength of CNTs while maintaining the electrical insulation of the polymer matrix, an effective solution is to cover the individual CNT with an insulating layer. [15-17] For example, Hayashida and coworkers pioneered the design of polymer based CNTs nanocomposite with a high electrical resistance by generating an insulating polymer layer on CNTs surface.[18] However, most of the former research [19-24] mainly focused on the preparation, electrically and thermally conductive properties of the nanocomposites filled with insulated CNTs. The important properties including mechanical, dielectric, and optical properties, as well as the practical applications in printed circuit substrates have been rarely investigated. Developing the CNTs filled polymer nanocomposites with high mechanical strength, electrical insulation and other excellent properties for practical applications still remains a challenge.

In this study, we developed a strategy for fabricating functionalized MWCNTs filled polymer nanocomposites with high mechanical strength and electrical insulation. The Functionalized MWCNTs were prepared by encapsulating MWCNTs with SiO_2 and the process was driven by the formation of Si-O-C bonds. Bismaleimide-triazine (BT) resin was employed as polymer matrix, which has been widely used in the printed circuit substrates due to its excellent thermal stability and good retention of mechanical properties at elevated temperatures.[25, 26] The results indicated that the obtained polymer nanocomposites possessed high mechanical strength, electrical insulation, improved thermal stability, a low dielectric constant of ~3.5 (1 GHz) and good optical transparency. The nanocomposites have been successfully applied to fabricate a printed circuit substrate,

on which a frequency "flasher" worked well. These unique properties were discussed based on the analysis of the microstructure and interfaces of the prepared nanocomposites.

2. Experimental

2.1 Materials

Tetraethyl orthosilicate (TEOS), ammonia solution (NH_4OH) (56 wt%), nitric acid (HNO_3), absolute ethanol (CH_3CH_2OH) and methyl ethyl ketone were acquired from Sinopharm Chemical Reagent Co., Ltd. MWCNTs prepared by a chemical vapor deposition (CVD) method were purchased from Carbon Nanotechnology Inc. China. Deionized water was produced by a Milli-QSystem (Millipore). 2,2'-bis (4-cyanatophenyl) propane (BCE, Heijang Kinlyuan Pharmaceutical Co., Ltd., China), 4,4'-bismaleimidodiphenylmethane (BMI，Honghu Bismaleimide Resin Factory, China), and 2, 2'diallyl bisphenol A (DBA, Wuxi Resin Factory, China) were used as starting materials to prepare the BT resin, according to our previous work.[27] All of the aforementioned reagents were of analytical grade and were used as received.

2.2 Oxidation of MWCNTs

MWCNTs (0.22 g) were modified by treating them in ~15.0 $mol.L^{-1}$ HNO_3 solution (40 mL) under reflux at 120 °C for 6 h. After cooling to room temperature, they were vacuum-filtered through a 0.45 mm polytetrafluoroethylene (PTFE) membrane and washed with deionized water until the filtrate reached a neutral pH. The oxidized MWCNTs were dried under vacuum for 24 h.

2.3 Preparation of MWCNT@SiO_2

The preparation of MWCNT@SiO_2 was based on MWCNTs-COOH via sol-gel reaction, as reported previously.[16] Oxidized MWCNTs (0.20) and ammonia solution (1.0 mL) were sonicated in ethanol/deionized water mixture (8:2 v/v, 100 mL) for 1 h. The pH of the mixture was kept at 11. In parallel, TEOS (2.0 mL) was sonicated in ethanol (40 mL) for 30 min. The TEOS/ethanol mixture was added dropwise to the oxidized MWCNTs solution. The reaction at 30 °C lasted for 2 h after addition of TEOS. The products were vacumm-filtered through a 0.45 μm PTFE membrane, and washed with absolute ethanol at least 5 times before drying at 80 °C for 12 h.

2.4 Preparation of polymer nanocomposites

The polymer nanocomposites were fabricated by solution processing. A certain amount of MWCNT@SiO_2 particles dispersed in methyl ethyl ketone were ultrasonicated to form a stable colloid, followed by adding a certain amount of BT resin and stirring for 4 h. Then a little hardener (2-ethyl-4-methylimidazole) was added and the mixture was stirred for another 2 h. Finally, the resultant solution mixture was coated onto the copper, and then dried at 100 °C for 2 h to thoroughly evaporate the solvent. The nanocomposites were then cured at 150 °C for 2 h, 180 °C for 2 h, and 200 °C for 2 h in sequence. The thickness of the nanocomposites was about 30 μm. A series of BT/MWCNT@SiO_2 nanocomposites were prepared with the MWCNT@SiO_2 loading varied between 0.4 and 2.0 wt%. For comparison studies, pure BT resin and nanocomposites filled with pristine MWCNTs and glass fibers were prepared via the same procedure.

2.5 Measurements

The morphology of the MWCNT@SiO_2 was examined by transmission electron microscopy (TEM, G2 F20, FEI Tecnai) with an accelerating voltage of 200 kV. The FTIR spectra were obtained on a Bruker Vertex 70 with pure KBr as the background from 400 and 4000 cm^{-1}. UV-vis spectra were performed with a UV-vis spectrometer (UV-3600, Shimadzu). Raman spectra were obtained from 1200 to 3000 cm^{-1} using a Raman spectrometer (Renishawin Via Raman microscope, excitation at 514 nm). The chemical state of the surface was characterized by X-ray photoelectron spectroscopy (XPS) on an Axis Ultra-DLD spectrometer (Kratos Analytical Ltd.), by using a monochromatized Al Ka source (1486.6 eV) operating at 15 kV and 15 mA. The vacuum during analysis was in the range from10^{-10} to 10^{-9} Pa. The Peakfit software was used to carry out the curve fitting. The volume resistivities of BT/MWCNT@SiO_2 and BT/MWCNT nanocomposites were measured using a high-resistance meter (Agilent 4339B, Agilent Technologies) and resistance meter (Keithley 2400, Keithley Instruments), respectively. The dielectric properties were measured with an impedance analyzer (Agilent 4991A) in the frequency range of 10^7-10^9 Hz. Static uniaxial in-plane tensile tests were conducted with a dynamic mechanical analyzer (DMA Q800, TA Instruments). The samples were cut with a razor into rectangular strips of approximately 4×15 mm^2 for mechanical testing. All tensile tests were conducted in controlled force rate mode with a preload of 0.001N and a force ramp rate of 1.0 $N.min^{-1}$. SEM images were obtained using a field-emission scanning electronmicroscope (Nova NanoSEM 450, FEI) combined with energy dispersive spectrometer (X-Max50, Oxford Instruments) with 5 or 10 kV accelerating voltage. Thermal stabilities of the nanocomposites were measured with a Thermogravimetric analysis (TGA, Thermal Analysis (TA) Instruments SDT-Q600 analyzer) in the air environment. The temperature ramps were from 40 to 900 °C at a heating rate of 10 $°C.min^{-1}$. A frequency "flasher" circuit was fabricated by bonding discrete electronic components to the MWCNT@SiO_2 nanocomposite film (100×50 mm^2) to demonstrate its potential application in printed circuit substrates.

3. Results and discussion

3.1 Characterization of MWCNT@SiO_2

The TEM examination (Figure 1a) reveals that there are almost no free SiO_2 particles in MWCNT@SiO_2 fillers. This is attributed to the generation of oxygenated groups on MWCNTs by acid treatment, which facilitates the heterogeneous nucleation of SiO_2 on MWCNT surfaces while inhibiting its homogeneous nucleation. In other words, oxidization process of MWCNT promotes the formation of SiO_2 shell on its surface rather than growing into free SiO_2 particles. The amorphous SiO_2 layer with ~ 10 nm in thickness is uniformly coated on the surface of MWCNT, as shown in Figure 1b and c, and SEM images (Figure S1, ESI†). In addition, the energy dispersive X-ray spectroscopy (EDX) elemental mappings (Figure S2, ESI†) of carbon, silicon, and oxygen further confirm that SiO_2 is uniformly coated onto

MWCNTs. The calculated SiO_2 weight loading in MWCNT@SiO_2 is 22.8%. Surface functionalization of MWCNT is expected to have a significant effect on its dispersibility in water. Indeed, the MWCNT@SiO_2 in water exhibits good dispersion, whereas the pristine MWCNTs deposit at the bottom, as shown in Figure 2(d). Moreover, the MWCNT@SiO_2 shows higher light transmittance compared with MWCNTs-COOH with the same loading in water.

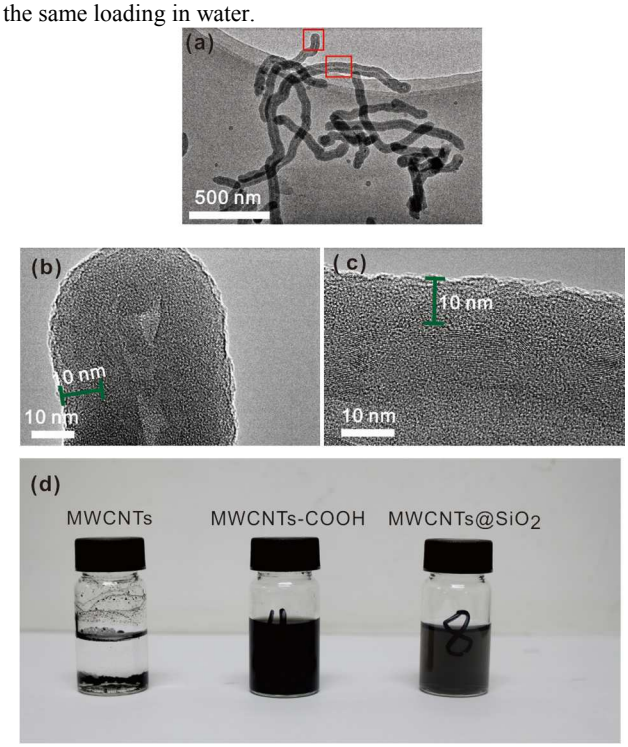

Figure 1. TEM images of (a) MWCNT@SiO_2; (b) and (c) are the enlarged ones of the selected regions in (a); (d) photograph of pristine MWCNTs, CNTs-COOH and MWCNT@SiO_2 dispersed in water.

The existence of functional groups in the MWCNT@SiO_2 is evidenced by FTIR (Figure 2). The characteristic absorption bands of MWCNTs@SiO_2 at approximately 1109, 957, 798 and 476 cm^{-1} are ascribed to υ_{as} (Si-O-Si), υ(Si-OH), υ(Si-O-Si), and δ(Si-O-Si), respectively, indicating the formation of SiO_2 on MWCNTs. The peak at 3414 cm^{-1} is assigned to the O-H stretches of Si-OH, which may be beneficial to improve the MWCNT@SiO_2's interfacial interaction with polymer.

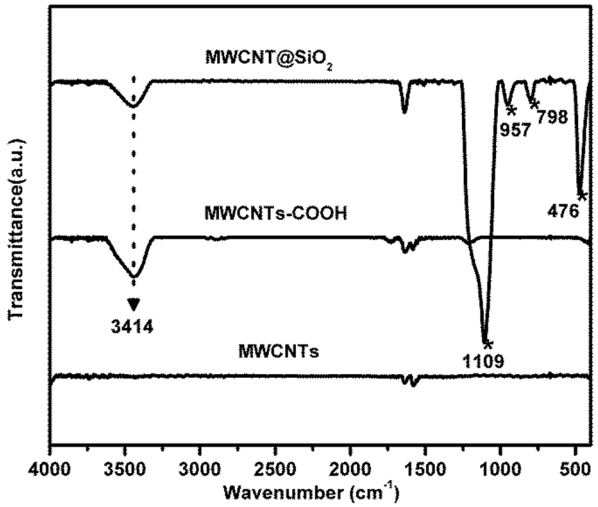

Figure 2. FTIR spectra of pristine MWCNTs, CNTs-COOH, and MWCNT@SiO_2.

To confirm the formation of a covalent bond between SiO_2 and MWCNT, XPS experiments were carried out, as shown in Figure 3 (a). The spectrum of C_{1s} electron orbital (Figure 3(b)), indicates the existence of seven carbon components: the graphite (283.3 ev), the C_{sp2} (284.8 ev), the C_{sp3} (285.1 ev), the C-O bond (287.1 ev), the C=O bond (287.8 ev), the O=C-O bond (289.0 ev), and the carbon of π-π* (289.1). Through the fitting of the O 1s electron orbital spectrum (Figure 3(c)), the -O- (533.0 eV) are observed. The SiO_2 component at 104.2 ev in Si_{2p} electron orbital spectrum can be observed (Figure 3(d)). The presence of SiO_2-C_2 (101.1 eV) and SiO_3-C (103.6 eV) bonds indicates the existence of a covalent bond (Si-O-C) between SiO_2 and MWCNT.

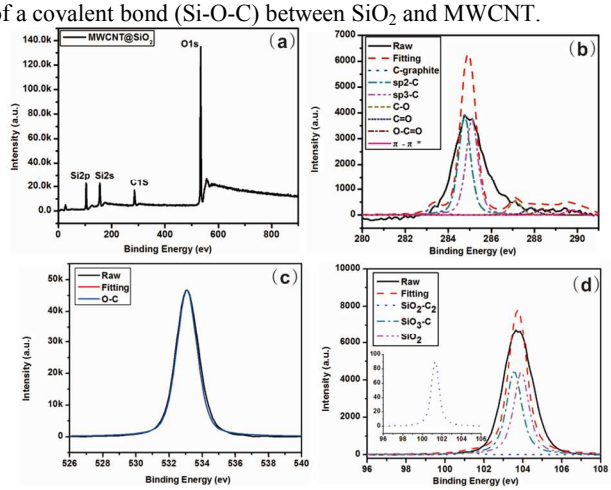

Figure 3. XPS spectra of MWCNT@SiO_2 (a); high resolution scans of C_{1s} region (b), O_{1s} region (c), and Si_{2p} region (d) of MWCNT@SiO_2.

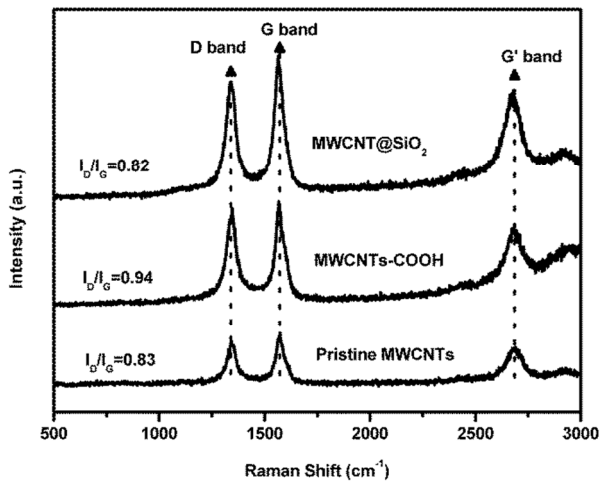

Figure 4. Raman spectra of pristine MWCNTs, CNTs-COOH, and MWCNTs@SiO_2.

Figure 4 presents Raman spectra of the MWCNTs@SiO_2. The MWCNTs and functionalized MWCNTs (MWCNTs-COOH and MWCNT@SiO_2) exhibit a D band at around 1340 cm^{-1}, which is induced by the disordered structure or sp^3 hybridized carbons and a G band at around 1570 cm^{-1}, which is derived from the splitting of the E_{2g} stretching mode of graphite. The intensity ratio of D band and G band (I_D/I_G) is used to characterize the defect quantity and monitor the functionalization of carbon materials. In our work, due to increasing defects and new edges introduced during the oxidative treatment, the value of I_D/I_G increased from 0.83 (pristine MWCNTs) to 0.94 (MWCNTs-COOH). After encapsulating MWCNT with SiO_2, I_D/I_G of CNT decreased to 0.82, even slightly lower than that of the pristine MWCNTs. These results can be interpreted in terms of some defect suppression of the lattice after coating SiO_2.

3.2 Properties of BT/MWCNT@SiO_2 nanocomposites

Optical property

Figure 5(a) presents photographs of the BT/MWCNTs@SiO_2 and BT/MWCNTs nanocomposite films with different loadings. The BT/MWCNT@SiO_2 nanocomposite films are optically transparent at all filler loadings and their light transmittance at 800 nm is about 30%, which is slightly lower than that of the neat BT resin film (37%). In contrast, the light transmittance rate of the BT/MWCNTs nanocomposite films significantly decreases with increasing pristine MWCNTs loadings (Figure 5(b)). When the pristine MWCNTs loading is 1.6 wt%, the light transmittance of the composite is only 5%. The enhanced optical transmittance compared with pristine MWCNTs should be originated from the uniform dispersion of MWCNT@SiO_2 in BT resin and the SiO_2 layer, which can prevent the light absorption of MWCNTs. The transparent property of materials is very important, especially for the applications in flexible displays, colourful e-paper, organic light-emitting diodes (OLEDs) and organic photovoltaics (OPVs). It is assumed that this strategy may be extended to fabrication of nanocomposites filled with MWCNT@SiO_2 with higher transparency by proper choice of polymers, and thus broaden the application of MWCNT@SiO_2.

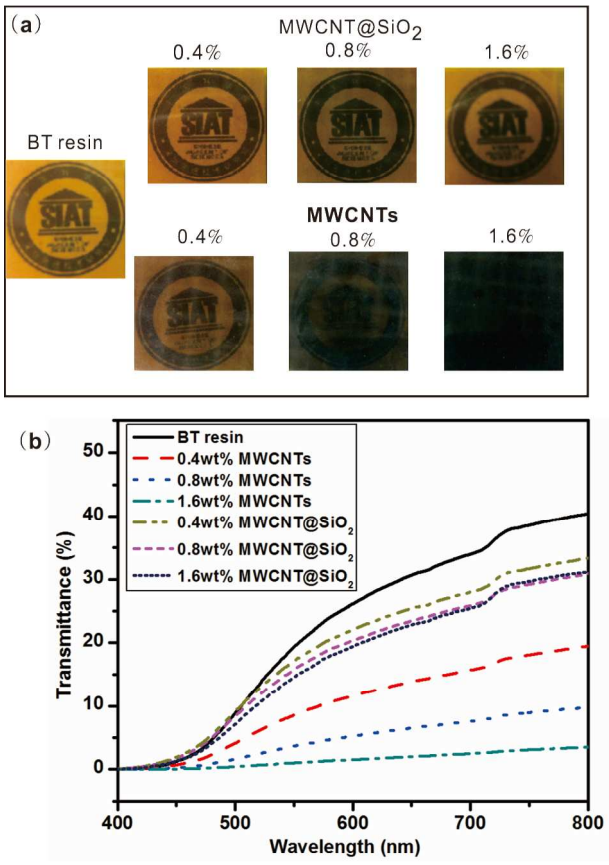

Figure 5. The effect of MWCNT@SiO_2 on the optical transparency and UV-vis transmittance of the nanocomposite films: (a) photographs showing the transparency of samples; (b) UV-vis spectra of nanocomposites with different MWCNT and MWCNT@SiO_2 loadings.

Electric and dielectric properties

Figure 6 shows the volume resistivity of the BT/MWCNT@SiO_2 and BT/MWCNT nanocomposites with different filler loadings. Addition of a small amount of pristine MWCNTs (0.4 wt%) leads to the transformation of the nanocomposite from insulator to semiconductor. Specifically, the volume resstivity declines from 1.32×10^{17} Ω.cm for pure BT resins to 6.14×10^4 Ω.cm for the nanocomposite containing 0.8 wt% MWCNTs. In contrast, the insulate SiO_2 coated on MWCNT surface exhibits a barrier effect on the electrons transformation. The volume resistivity of the nanocomposites containing MWCNT@SiO_2 is higher by approximately five orders of magnitude than that containing the pristine MWCNTs, at the same loadings. When the MWCNT@SiO_2 loading is 0.8 wt%, the measured volume resistivity of the nanocomposite is 2.36×10^9 Ω.cm, indicating that it is still an insulator (>1.0×10^9 Ω.cm). However, further increase of MWCNT@SiO_2 loading leads to a decrease of volume resistivity to 4.74×10^7 Ω.cm, suggesting that the nanocomposite is not insulated.

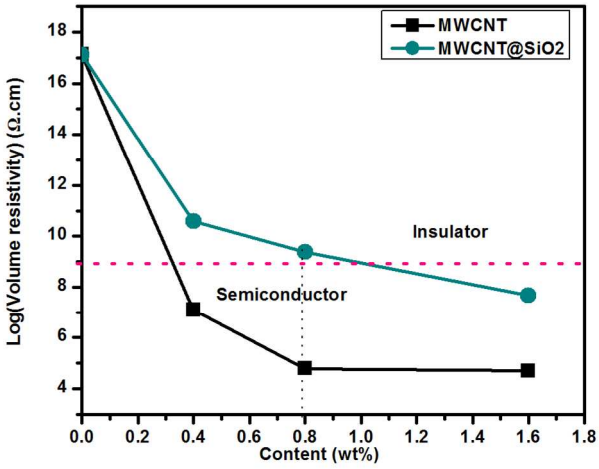

Figure 6. Volume resistivity of BT/MWCNT and BT/MWCNT@SiO_2 nanocomposites with different filler loadings.

The miniaturization of electronic devices integrated in printed circuits substrates has resulted in rapid increase of the propagation delay caused by interconnection. In order to reduce the resistance-capacitance (RC) delay, low dielectric constant and loss of insulating materials are urgently desired.[28] As shown in Figure 7 (a) and (b), all nanocomposites show similar dielectric stability on frequency and their dielectric constants increase linearly with loading amount. Compared to the pristine MWCNTs (Figure 7 (c)), MWCNT@SiO_2 leads to less improvement in the dielectric constant of BT resin. With the same loading (1.6 wt%), the dielectric constant of BT/MWCNT@SiO_2 nanocomposites increase from 3.0 for pure BT resin to 3.5, while it increases to 5.0 for BT/MWCNTs nanocomposites. On the other hand, it seems that the addition of MWCN@SiO_2 does not influence the dielectric loss of BT resin. In contrast, the dielectric loss of the BT/MWCNTs nanocomposites (Figure 7(d)) increases with filler loading and reaches up to 0.04. We also find that adding more MWCNT@SiO_2 (2.0 wt%) leads to increased dielectric loss (0.04) (Figure S3, ESI†), which may be attributed to the poorer dispersion of MWCNT@SiO_2 in BT resins, which causes the regional formation of a conductive network of the CNT within the polymer matrix. There are two possible explanations for the discrepancy of dielectric properties between MWCNT@SiO_2 and MWCNT. First, the insulated SiO_2 layer on MWCNT limits the dipoles moment, resulting in low energy storage in an electromagnetic field. Second, dielectric properties depend on the inter-action between inorganic and polymer. Because MWCNT@SiO_2 has stronger inter-action with BT resin than pure MWCNTs due to the existence of active -OH group, MWCNT@SiO_2 fillers have bigger restricting influence on the orientation and relaxation of dipoles than MWCNTs in nanocomposites.

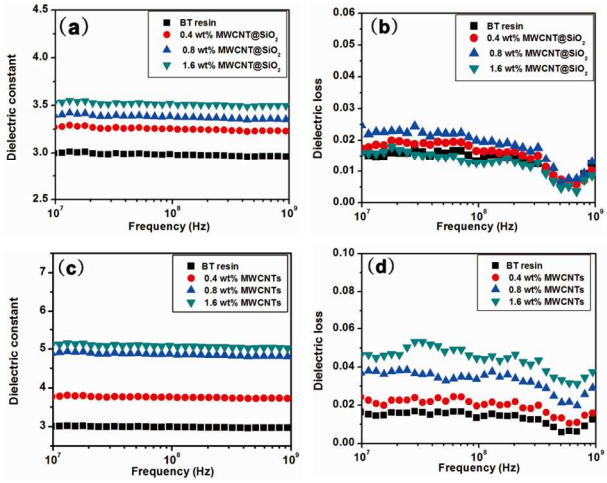

Figure 7. Dielectric constant and loss of BT/MWCNT@SiO_2 (a, b) and BT/MWCNT (c, d) with different filler loadings.

Mechanical properties

Figure 8(a) shows the typical stress-strain curves of BT/MWCNT@SiO_2 nanocomposites. The stress strength (Figure 8(b)) and ultimate strain (Figure 8(c)) were extracted from the curve just before failure. Young's modulus (Figure 8(d)) was calculated from the slope of the linear fit in the initial section of the curve (0.5 % strain). For the neat BT resin film, the stress strength, elongation and Young's modulus are 48.2 MPa, 2.6% and 1.6 GPa respectively. After the addition of pristine MWCNTs or MWCNT@SiO_2, the mechanical properties of BT resin increase with the filler loadings, and the addition of 0.8 wt% fillers exhibits the highest stress strength and elongation. Adding more fillers brings about a slight decrease in stress strength and elongation. Such a phenomenon was also observed in other reports.[29, 30] There could be regional agglomeration of the filler particles in the composite, which limits the efficiency of reinforcement. As compared to the pristine MWCNTs, MWCNT@SiO_2 leads to more pronounced improvement in the mechanical properties, except for the elongation values. The stress strength and Young's modulus of the nanocomposite containing 0.8 wt% MWCNT@SiO_2 are 87.4 MPa and 3.18 GPa, respectively, which are higher than that of the BT/pristine MWCNTs. Figure 8(d) displays that the elongation values of BT/MWCNT@SiO_2 are lower than those of the BT/MWCNTs composites, but still higher than that of pure BT resin. The results indicate strong interfacial interaction between MWCNT@SiO_2 and BT resin, which leads to difficult deformation of the nanocomposites under the tensile loading. Furthermore, as a control experiment, we also measured the mechanical properties of the composite filled with 0.8 wt% glass fibers which are the conventional composites used as printed circuit substrate materials. As shown in Figure 8, its tensile strength, elongation and Young's modulus are 63.0 MPa, 2.4 GPa, and 3.1%, respectively, which are all lower that of the nanocomposite filled with 0.8 wt% MWCNT@SiO_2. The control experiments with pristine MWCNTs and glass fibers confirm that MWCNT@SiO_2 plays the key role for enhancement of mechanical properties of BT resins.

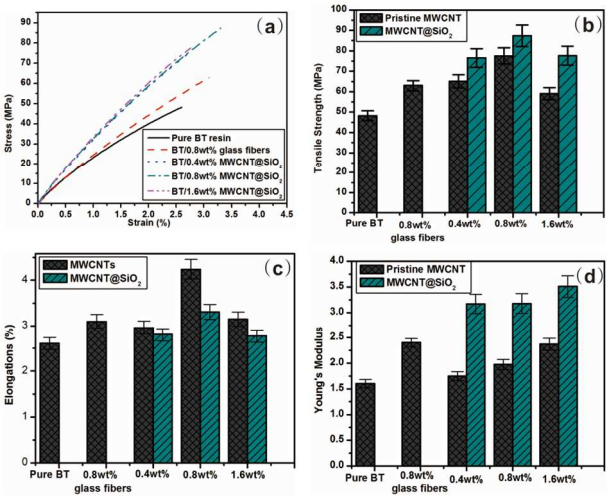

Figure 8. (a) typical stress-strain curves of BT resin based nanocomposites with different loadings of MWCNT@SiO_2 or MWCNTs, (b) absolute value of tensile strength, (c) percentage elongation, and (d) Young's modulus of the nanocomposites.

In order to compare the mechanical properties of the nanocomposites filled with functionalized CNTs, we define the rate of increase of tensile strength (σ) and Young's modulus (Y) to the CNTs' weight fraction (W). The equations are as followed:

$$\frac{d\sigma}{dW} = \frac{\sigma_C - \sigma_P}{W} \quad (1)$$

$$\frac{dY}{dW} = \frac{Y_C - Y_P}{W} \quad (2)$$

Table 1 summarizes recent typical studies on the effects of functionalized CNTs on the mechanical properties of polymer nanocomposites. These results indicate that the addition of functionalized CNTs can enhance the tensile strength and Young's modulus, and different systems possess different degree of mechanical improvement. In our research, the dσ/dW and dY/dW are as high as 4900 and 200, respectively, which are higher than most reported values. Therefore, we believe that the improvement of 81.2% and 98.5% in both tensile strength and Young's modulus in our results is significant.

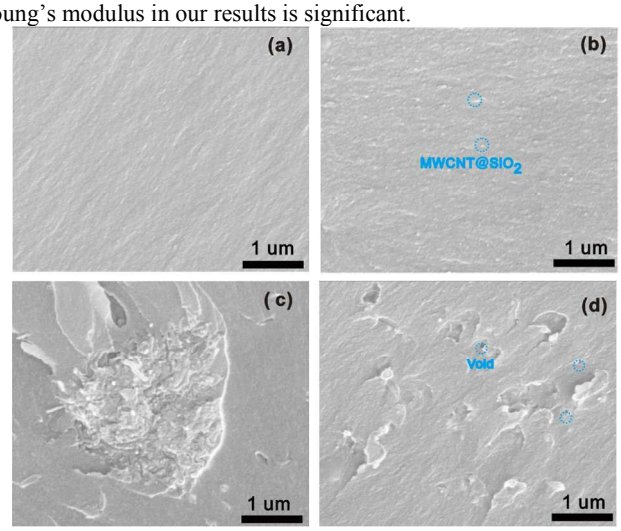

Figure 9. SEM fractographs of the pure BT resin and BT/MWCNTs@SiO_2 nanocomposites: (a) the pure BT resin; (b) 0.8 wt% MWCNT@SiO_2; (c) 0.8 wt% Pristine MWCNTs and (d) 1.6 wt% MWCNT@SiO_2.

Table 1. Comparison of mechanical properties of polymer nanocomposites between our BT/MWCNT@SiO_2 nanocomposite with the data from literature.

System [a]	CNTs loading	dσ (MPa)	dY (GPa)	dσ/dW	dY/dW	Reference and year
BT/MWCNT@ SiO_2 (this study)	**0.8 wt%**	**39.2**	**1.6**	**4900**	**200**	-
PMMA/f-MWCNTs	0.5 wt%	20.6	1.2	4120	240	[29]2012
Epoxy/f-SWNTs	0.5 wt%	34.4	0.5	6880	100	[31]2011
Epoxy/f-SWNTs	4.0 wt%	19	1.4	475	35	[32]2004
Epoxy/f-SWNTs	1.0 wt%	10.6	0.7	1060	73	[33]2008
Epoxy/f-MWNTs	5.0 wt%	Negligible	0.6	-	12	[34]1998
Epoxy/f-MWCNTs	6.0 wt%	Decrease	1.38	Decrease	23	[35]2004
Epoxy/f-MWCNTs	1.0 wt%	11	1.2	1100	120	[36]2003
Epoxy/f-MWCNTs	0.25 wt%	20	0.6	8000	240	[37]2008
Vulcanized rubber/f-SWCNTs	~1.0 wt%	4.5	0.46	450	46	[38]2007
polyurethane/f-SWCNTs	0.7 wt%	7	14.2	1000	2028	[39]2006

[a] PMMA: Poly(methyl methacrylate); f-SWNTs: functionalized single-walled carbon nanotubes; f-MWCNTs: functionalized multi-walled carbon nanotubes.

As we all know, the mechanical reinforcement of MWCNT filled nanocomposites strongly depends on the extent of load transfer between the matrix and MWCNTs.[31, 40, 41] For MWCNT@SiO_2, a number of OH groups have been verified to be attached to its surface, while pristine MWCNTs lack surface functional groups, as indicated in Figure 2. Therefore, the MWCNT@SiO_2 has stronger interfacial interactions with BT resins than pristine MWCNTs. These innate advantage results in efficient stress transfer between the MWCNT@SiO_2 and BT matrix, which could avoid the deformation or fracture of the materials under external force. On the other hand, the dispersion of nanofiller in matrix is another key factor that affects the reinforcement. As shown in SEM images in Figure 9(a), the pure BT resin exhibits a smooth fracture surface. After the addition of MWCNT@SiO_2 (0.8 wt%) into BT resin, MWCNT@SiO_2 are well-dispersed in the nanocomposites, as shown in Figure 9(b). In contrast, the agglomeration or voids can be clearly seen in BT/MWCNTs nanocomposite with the same nanofiller loading

(Figure 9(c)). Owing to the good dispersion of MWCNT@SiO_2 in the matrix, the large surface area enables more interaction sites at the polymer/nanofiller interphase, leading to the improved mechanical strength. With the higher loading of 1.6 wt%, the composite exhibits a significantly increased viscosity, so that porosity is easily introduced to the composite, as shown in Figure 9(d). The tensile strength of composites is very sensitive to such void defects. Therefore, a slightly decreased tensile strength is observed for the composite with the addition of 1.6 wt% MWCNT@SiO_2.

Thermal stability

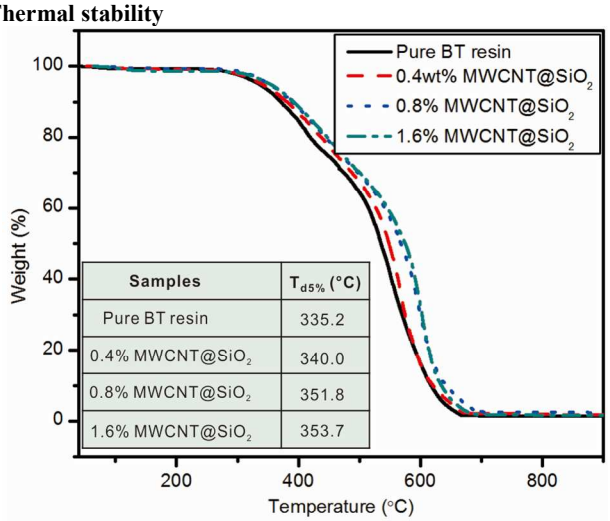

Samples	$T_{d5\%}$ (°C)
Pure BT resin	335.2
0.4% MWCNT@SiO_2	340.0
0.8% MWCNT@SiO_2	351.8
1.6% MWCNT@SiO_2	353.7

Figure 10. TGA curves of the pure BT resin and nanocomposites containing different MWCNT@SiO_2 loadings. The inset shows the $T_{d5\%}$ values for all samples.

Thermal stability is one of the most important properties of the nanocomposites to assess their processing and service-life performance in the applications of printed circuit substrates. Figure 10 shows the TGA curves for the pure BT resin and BT/MWCNT@SiO_2 nanocomposites. The nanocomposites are stable up to 350 °C and then completely decompose at above 700 °C, leaving no residue. The 5 wt% weight loss temperatures ($T_{d5\%}$) for all samples are extracted and summarized in the inset of Figure 10. The values of $T_{d5\%}$ increase from 335.2 °C for the pure BT resin to 353.7 °C for the nanocomposite containing 1.6 wt% MWCNT@SiO_2, indicating the improved thermal stability. The stabilization effect of MWCNTs@SiO_2 is mainly attributed to good polymer matrix-MWCNT@SiO_2 interaction, as well as barrier effect of MWCNT@SiO_2. Furthermore, the growth of $T_{d5\%}$ slows down when MWCNT@SiO_2 is more than 0.8 wt%, due to the existence of agglomerations in the composite, as shown in the SEM image (Figure 9d).

4. Application in frequency ‘‘flasher’’circuit

In order to demonstrate the potential application of the BT/MWCNT@SiO_2 nanocomposites in printed circuit substrates, we fabricated a frequency “flasher” circuit by bonding discrete electronic components to our nanocomposite substrate. The MWCNT@SiO_2 loading in the nanocomposite is 0.8 wt%, which leads to the maximum values in mechanical properties as shown in the above results. One should note that the BT loaded with 0.8 wt% pristine MWCNTs cannot be used as the printed circuit substrate, because of its low electrical resistivity. In addition, the pure BT resin is also not the ideal circuit substrate because of its low mechanical strength, which will lead to easy break during the fabrication of the circuit.

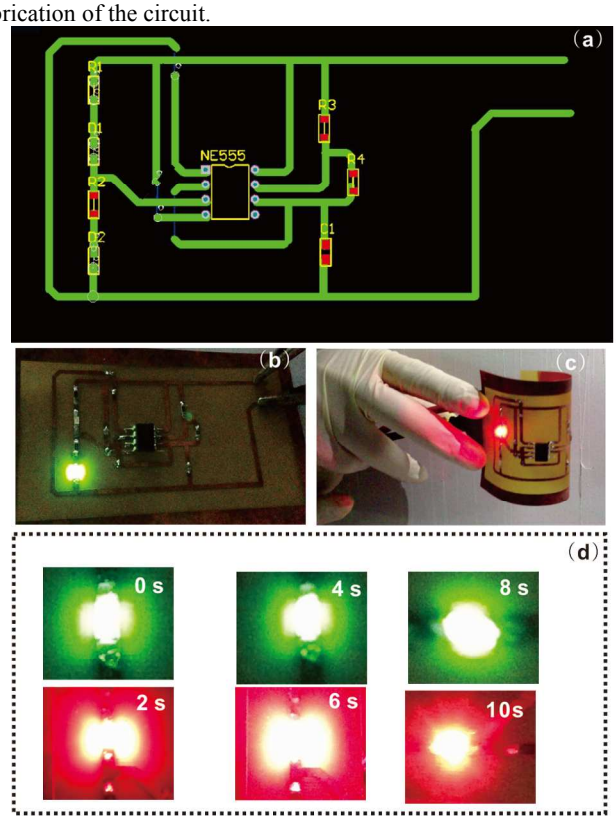

Figure 11. Applications of the nanocomposite in printed circuit substrates: (a) circuit principle diagram of FFC. (b, c) the optical images of FFC working before and after bending; (d) optical images of two LEDs flashed alternately.

Figure 11(a) presents the circuit principle diagram. The circuit comprises of four resistors (R1, R2, R3, and R4), one capacitor, one power (6 V), one 555 timer integrated circuit (NE555) and two LEDs (green (D1) and red (D2)). The detailed manufacturing process of the frequency “flasher” circuits follows that of the common printed circuit boards (PCB). The copper (Cu) clad laminate containing MWCNT@SiO_2 was prepared, so that we can use copper wire as electrical circuit. Figure S4 shows the fabrication process of the copper clad laminate. The electrical circuit was fabricated by UV photoengraving method (Figure S5, ESI†). The circuit could be turned on by connecting the negative and positive electrodes (Figure 11(b)). The working printed circuit substrate demonstrates excellent flexibility. As shown in Figure 11(c), it is working well after bending to a certain extent. When the circuit is on, the two LEDs flash alternately at a fixed frequency (Figure 11(d)). A movie of the operation of the LED chip can be found in the electronic supplementary information (see Movie S1, ESI†).

5. Conclusions

We have demonstrated a strategy for fabricating MWCNTs based polymer nanocomposites with high mechanical strength and electrical insulation by encapsulating MWCNT with SiO_2 (MWCNT@SiO_2). With only 0.8 wt% MWCNT@SiO_2, the resultant nanocomposites exhibits 81.2% and 98.5 % increases in

tensile strength and Young's modulus (compared to pure BT resin), respectively. The volume resistivity of the nanocomposites containing MWCNT@SiO_2 is higher by approximately five orders of magnitude than that containing the pristine MWCNTs at the same loadings. Addition of MWCNT@SiO_2 hardly affects the dielectric properties and optical transparency of BT resin. Furthermore, the values of $T_{d5\%}$ increase with increase of MWCNT@SiO_2, and reaches 353.7 °C for the nanocomposite containing 1.6 wt% MWCNT@SiO_2, which is 18.5 °C higher than that of pure BT resin. These excellent properties are attributed to MWCNT@SiO_2's strong interfacial interactions with BT resin and high electrical insulation of the SiO_2-coated MWCNTs. The BT/MWCNT@SiO_2 nanocomposites have been successfully demonstrated as a printed circuit substrate, on which a frequency "flasher" circuit and the electrical components worked well. The concept of using MWCNT@SiO_2 as fillers in this study will also be applicable to a wide range of other polymer nanocomposites.

ACKNOWLEDGMENT

The authors acknowledge the financial support from National Natural Science Foundation of China (No.51377157), Guangdong and Shenzhen Innovative Research Team Program (No. 2011D052 and KYPT20121228160843692) and Shenzhen Electronic Packaging Materials Engineering Laboratory (No.2012-372).

Notes and references

[a] *Shenzhen Institutes of Advanced Technology, Chinese Academy of Sciences.1068 Xueyuan Avenue, Shenzhen University Town, Shenzhen, China*

[b] *College of Advanced Technology, University of Chinese Academy of Sciences, China.*

[c] *Department of Electronics Engineering, The Chinese University of Hong Kong, Hong Kong, China*

*Corresponding authors. Email: Shuhui Yu, sh.yu@siat.ac.cn; Rong Sun, rong.sun@siat.ac.cn.

† Electronic Supplementary Information (ESI) available: [SEM images of MWCNT@SiO_2, EDX elemental mapping of MWCNT@SiO_2, dielectric properteis of BT/2.0 wt% MWCNT@SiO_2 nanocomposite, preparation of copper clad laminate containing MWCNT@SiO_2, fabrication of electrical circuit by subtractive process, and a video that shows the operation of the frequency "flasher" circuits.]. See DOI: 10.1039/b000000x/.

1. M. Naffakh, A. M. Díez-Pascual, C. Marco, G. J. Ellis and M. A. Gómez-Fatou, *Progress in Polymer Science*, 2013, **38**, 1163-1231.
2. J. N. Coleman, U. Khan and Y. K. Gun'ko, *Advanced Materials*, 2006, **18**, 689-706.
3. N. Roy, R. Sengupta and A. K. Bhowmick, *Progress in Polymer Science*, 2012, **37**, 781-819.
4. A. M. Diez-Pascual and D. Gascon, *ACS applied materials & interfaces*, 2013, **5**, 12107-12119.
5. Y. Ma, P. L. Chiu, A. Serrano, S. R. Ali, A. M. Chen and H. He, *Journal of the American Chemical Society*, 2008, **130**, 7921-7928.
6. N. G. Sahoo, S. Rana, J. W. Cho, L. Li and S. H. Chan, *Progress in Polymer Science*, 2010, **35**, 837-867.
7. C. Min, X. Shen, Z. Shi, L. Chen and Z. Xu, *Polymer-Plastics Technology and Engineering*, 2010, **49**, 1172-1181.
8. T. Souier, C. Maragliano, M. Stefancich and M. Chiesa, *Carbon*, 2013, **64**, 150-157.
9. J. Zhang, D. Jiang, H.-X. Peng and F. Qin, *Carbon*, 2013, **63**, 125-132.
10. E. Y. Li and N. Marzari, *ACS Nano*, 2011, **5**, 9726-9736.
11. S. L. Zhang, S. B. Yin, C. R. Rong, P. F. Huo, Z. H. Jiang and G. B. Wang, *Eur. Polym. J.*, 2013, **49**, 3125-3134.
12. X. Sun, H. Sun, H. Li and H. Peng, *Advanced materials (Deerfield Beach, Fla.)*, 2013, **25**, 5153-5176.
13. S. Desbief, N. Hergue, O. Douheret, M. Surin, P. Dubois, Y. Geerts, R. Lazzaroni and P. Leclere, *Nanoscale*, 2012, **4**, 2705-2712.
14. Y. Q. Li, Y. A. Samad, K. Polychronopoulou, S. M. Alhassan and K. Liao, *Scientific Reports*, 2014, **4**, 4652.
15. K. Ding, B. Hu, Y. Xie, G. An, R. Tao, H. Zhang and Z. Liu, *Journal of Materials Chemistry*, 2009, **19**, 3725-3731.
16. A. J. Paula, D. Stefani, A. G. Souza Filho, Y. A. Kim, M. Endo and O. L. Alves, *Chemistry-a European Journal*, 2011, **17**, 3228-3237.
17. S. W. Kim, T. Kim, Y. S. Kim, H. S. Choi, H. J. Lim, S. J. Yang and C. R. Park, *Carbon*, 2012, **50**, 3-33.
18. K. Hayashida and H. Tanaka, *Advanced Functional Materials*, 2012, **22**, 2338-2344.
19. S. K. Yadav, I. J. Kim, H. J. Kim, J. Kim, S. M. Hong and C. M. Koo, *Journal of Materials Chemistry C*, 2013, **1**, 5463-5470.
20. T. Morishita, M. Matsushita, Y. Katagiri and K. Fukumori, *Journal of Materials Chemistry*, 2011, **21**, 5610-5614.
21. W. Cui, F. Du, J. Zhao, W. Zhang, Y. Yang, X. Xie and Y.-W. Mai, *Carbon*, 2011, **49**, 495-500.
22. Y. Zhang, S. Xiao, Q. Wang, S. Liu, Z. Qiao, Z. Chi, J. Xu and J. Economy, *Journal of Materials Chemistry*, 2011, **21**, 14563-14568.
23. J. Di, Z. Yong, Z. Yao, X. Liu, X. Shen, B. Sun, Z. Zhao, H. He and Q. Li, *Small*, 2013, **9**, 148-155.
24. A. Gohier, B. Laik, K.-H. Kim, J.-L. Maurice, J.-P. Pereira-Ramos, C. S. Cojocaru and V. Pierre Tran, *Advanced Materials*, 2012, **24**, 2592-2597.
25. X. Zeng, S. Yu and R. Sun, *J. Appl. Polym. Sci.*, 2013, **128**, 1353-1359.
26. X. Zeng, S. Yu, R. Sun and R. Du, *Materials Chemistry and Physics*, 2011, **131**, 387-392.
27. X. L. Zeng, S. H. Yu and R. Sun, *J. Appl. Polym. Sci.*, 2013, **128**, 1353-1359.
28. C. Yuan, K. Jin, K. Li, S. Diao, J. Tong and Q. Fang, *Advanced Materials*, 2013, **25**, 4875-4878.
29. J. Wang, Z. Shi, Y. Ge, Y. Wang, J. Fan and J. Yin, *Journal of Materials Chemistry*, 2012, **22**, 17663-17670.
30. L. An, Y. Pan, X. Shen, H. Lu and Y. Yang, *Journal of Materials Chemistry*, 2008, **18**, 4928-4941.
31. J. M. Gonzalez-Dominguez, A. Anson-Casaos, A. M. Diez-Pascual, B. Ashrafi, M. Naffakh, D. Backman, H. Stadler, A. Johnston, M. Gomez and M. Teresa Martinez, *Acs Applied Materials & Interfaces*, 2011, **3**, 1441-1450.

32. J. Zhu, H. Peng, F. Rodriguez-Macias, J. L. Margrave, V. N. Khabashesku, A. M. Imam, K. Lozano and E. V. Barrera, *Advanced Functional Materials*, 2004, **14**, 643-648.
33. L. Sun, G. L. Warren, J. Y. O'Reilly, W. N. Everett, S. M. Lee, D. Davis, D. Lagoudas and H. J. Sue, *Carbon*, 2008, **46**, 320-328.
34. L. S. Schadler, S. C. Giannaris and P. M. Ajayan, *Applied Physics Letters*, 1998, **73**, 3842-3844.
35. Y. Breton, G. Désarmot, J. P. Salvetat, S. Delpeux, C. Sinturel, F. Béguin and S. Bonnamy, *Carbon*, 2004, **42**, 1027-1030.
36. J. Bai, *Carbon*, 2003, **41**, 1325-1328.
37. Y. Geng, M. Y. Liu, J. Li, X. M. Shi and J. K. Kim, *Composites Part A: Applied Science and Manufacturing*, 2008, **39**, 1876-1883.
38. A. M. Shanmugharaj, J. H. Bae, K. Y. Lee, W. H. Noh, S. H. Lee and S. H. Ryu, *Composites Science and Technology*, 2007, **67**, 1813-1822.
39. H. Xia and M. Song, *Journal of Materials Chemistry*, 2006, **16**, 1843-1851.
40. Z. Chen and H. Lu, *Journal of Materials Chemistry*, 2012, **22**, 12479-12490.
41. D. Ciprari, K. Jacob and R. Tannenbaum, *Macromolecules*, 2006, **39**, 6565-6573.

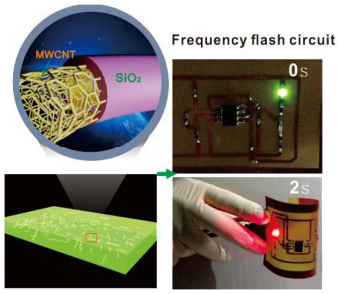

Functionalized multiwalled carbon nanotubes (MWCNTs)-silicon oxide (SiO_2) core-shell nanoparticles filled polymer nanocomposites with high mechanical strength and electrical insulation were developed, and employed to fabricate a printed circuit substrate.